

Copyright  
by  
Jessica Caitlin Treff  
2011

**The Thesis Committee for Jessica Caitlin Treff  
Certifies that this is the approved version of the following thesis:**

**IGF-1 conjugated to a PEGylated-Fibrin hydrogel as a therapeutic  
modality for eccentric muscle damage in rats**

**APPROVED BY  
SUPERVISING COMMITTEE:**

**Supervisor:**

---

Roger P. Farrar

---

Laura J. Suggs

**IGF-1 conjugated to a PEGylated-Fibrin hydrogel as a therapeutic  
modality for eccentric muscle damage in rats**

**by**

**Jessica Caitlin Treff, B.S.**

**Thesis**

Presented to the Faculty of the Graduate School of

The University of Texas at Austin

in Partial Fulfillment

of the Requirements

for the Degree of

**Masters of Science in Kinesiology**

**The University of Texas at Austin**

**December 2011**

## **Acknowledgements**

I would like to thank Dr. Roger Farrar for his knowledge and guidance over the past two years. I would also like to thank David Hammers for his good ideas and technical support.

On a personal note, the opportunity to pursue higher education and learn about things that interest me would have never arisen if my parents had not encouraged and allowed me to do what I thought best. They did not care which direction I took, as long as it challenged me and made me happy.

I must thank my fiancé, who enjoys science just as much as I do. He kept me balanced throughout this whole endeavor, moved away from the mountains to be near me and has waited for me to finish this period of my life so that we could start a new chapter together.

Lastly, though science is science and religion is religion, I could not have completed this science without the divine oversight of my Lord.



## **Abstract**

### **IGF-1 conjugated to a PEGylated-Fibrin hydrogel as a therapeutic modality for eccentric muscle damage in rats**

Jessica Caitlin Treff, M.S.Kin.

The University of Texas at Austin, 2011

Supervisor: Roger P. Farrar

We evaluated the efficacy of treating eccentric muscle damage with IGF-1 PEGylated to a fibrin biomatrix. With one injection, delivered one hour after the induction of eccentric muscle damage we saw an attenuation of force loss early in recovery, maintenance of muscle weight, and progression to the repair/regeneration of the damaged fibers at a greater speed and magnitude in the first week of recovery. As opposed to introducing an unbound bolus of IGF-1, we believe the ability of the PEGylated-fibrin to stabilize and sustain delivery of the molecule results in significantly better recovery. Coupling IGF-1, which has multiple beneficial effects in tissue repair, with this system of delivery provides a simple and easy to administer treatment for eccentric muscle damage. With this form of damage being the most prevalent of all skeletal muscle damage types, since it underlies all muscle strain, a simple and effective treatment is important for increasing functional recovery after injury.

## Table of Contents

List of Figures and Tables.....	viii
INTRODUCTION .....	1
RELATED LITERATURE.....	4
Eccentric Skeletal Muscle Damage & Repair.....	4
IGF-1 in Repair and Regeneration .....	7
PEGylated-Fibrin Biomatrix as a Delivery System for IGF-1.....	9
SIGNIFICANCE OF STUDY .....	13
METHODS .....	14
Biomatrix Preparation .....	14
Induction of Eccentric Damage .....	15
Functional Analysis .....	16
Histological Analysis .....	17
Imaging and Analysis .....	18
Statistical Analysis.....	18
RESULTS .....	19
Western Blot .....	19
Functional .....	19
Morphological.....	20
Histological .....	21
Figures.....	23
DISCUSSION .....	32
APPENDICES .....	35
A: Biomatrix Preparation .....	35
B: Biomatrix Protein Analysis .....	36
C: Induction of Eccentric Damage.....	41

D: Force Measurement and Tissue Harvest .....	44
E: Histological Analysis .....	45
F: Raw Morphometric and Functional Data .....	46
REFERENCES .....	49
VITA.....	52

## List of Figures and Tables

Figure 1. Western blotting with anti-IGF-1 antibody (dark stain) verifies covalent linkage of IGF-1 on PEG-Fib biomatrix. The largest complexes were found in the PEG + Fib + IGF-1 lane with the protein sizes above 250 kDa according to the protein size ladder in the first lane. ....	23
Table 1. Dry weight of TA expressed as a percentage of wet weight. No significance differences were. Trend observed in dry weight percentage increasing from 3 to 7 days of recovery. ....	23
Table 2. Morphometric and functional data expressed as mean (SD). Physiological cross sectional area (PCSA), Maximal isometric tetanic force (Po), Specific tension (sPo). Control values were pooled from all control legs. a significantly different from control, b significantly different from treatment pair, c significantly different from time-matched PFI. ....	24
Table 3. Morphometric and functional data expressed as a percentage of the contralateral control. a significantly different from control, b significantly different from treatment pair, c significantly different from time-matched PFI. ....	24
Figure 2. <i>In situ</i> measure of maximal force generation (N) of recovering muscle, expressed as percent of contralateral control force. Brackets indicate p-values < 0.01. ....	25
Figure 3. Weight change after injury, expressed as percentage of contralateral control weight. Brackets indicate p-values < 0.005. ....	25
Figure 4. Mean fiber size of control and treatment groups ( $\mu\text{m}^2$ ) with SD. ....	26

Figure 5. Myofiber size distribution at 3 days post-injury. Control fiber sizes seen in gray, experimental fiber sizes in black. ....	27
Figure 6. Myofiber size distribution 7 days post injury. Control fiber sizes seen in gray, experimental fiber sizes in black. ....	28
Figure 7. Histological evaluation of fibers with H&E staining. (A) represents uninjured tissue, (B), (C) and (D) represent tissue 3 days post injury, (E), (F) and (G) represent tissue 7 days post-injury. (B) and (E) are PBS treated, (C) and (F) are PF treated, and (D) and (G) were treated with PFI. Viewed with 20x objective power. Scale bar = 100µm. ....	30
Figure 8. Example of centrally nucleated fibers (black rectangles) from the PFI 7 muscle seen in Figure 7. Viewed with 20x objective power. Scale bar = 100 µm. ....	30
Figure 9. H&E staining was used to determine the percentage of the total fibers with centralized nuclei. All groups were significantly above control value. All treatment pairs had p-values < 0.001. Brackets within recovery time groups indicate p-values < 0.05. ....	31

## INTRODUCTION

The science of tissue repair is complex. Though it is similar among the tissues of the human body, it's complexity lies in the precise orchestration of chemical and cellular components throughout the body. The effectiveness of our innate tissue repair systems requires the production of many types of chemokines and proteins in the right amount, at the right time, and in a specific area to meet the minimum requirements of cellular recruitment and differentiation to carry out regeneration of tissue. Many types of tissue damage can exceed the capabilities of this innate system resulting in scarring or loss of functionality, and time lost to injury. Medicine has long sought treatments that enhance and speed the natural process, with the best treatment being one that could be applied to any tissue and be modified to bolster the chemical or cellular response. The question of when, what and how much of a component to introduce to a damaged site is currently being answered and will continue to be answered for decades. A simpler problem to pursue is how to deliver the treatment, particularly how to intervene without interfering with this intricate system.

Within the last six years, a product has been introduced that incorporates fibrin and poly(ethylene glycol), two biomaterials that have been used in other FDA approved biomaterials, into an injectable hydrogel substance that has been used to deliver cells and important proteins to damaged tissues (Zhang G 2006, Hammers 2011). The PEGylated-fibrin biomatrix has met the requirements of being biocompatible and biodegradable (Drinnan 2010). It is multifunctional, in that it can be used to release different proteins at

different rates or to introduce progenitor or other cell types to precise areas of tissues (Zhang 2006, Drinnan 2010). Since it is a recent discovery, it's potential has not been fully elucidated. It has proven effective as a delivery system when used to introduce bioactive molecules to cell populations to stimulate proliferation and differentiation, as a delivery system for mesenchymal stem cells and stromal derived factor-1 after myocardial infarction, and as a delivery system for insulin-like growth factor-1 (IGF-1) to ischemia/reperfused skeletal muscle (Zhang 2006, 2007, 2008, Drinnan 2010, Hammers 2011). It has great potential to be applied to many tissue damage models. With this study, we tested its applicability to the common type of skeletal muscle damage, eccentric damage.

Eccentric muscle damage can be incurred in any physical activity, especially where rapid deceleration of a joint or overextension of a muscle occurs, and is involved in the disease muscular dystrophy (Allen 2001). It is thought to be the most common form of muscle injury because it is the mechanism that underlies all forms of muscle strain. It is especially prevalent in the muscle injury of people unaccustomed to eccentric contractions, such as sedentary and ageing individuals (Brooks 1990). It involves mechanical strain that disrupts the contractile proteins and membranes of muscle cells (Friden and Lieber 2001). We used this model to test the acute effects to recovery of IGF-1, delivered by the PEGylated-fibrin biomatrix.

The IGF-1 molecule that we delivered to the damaged tissue has many beneficial effects. It stimulates protein synthesis, cell survival and enhanced satellite cell response

in muscle regeneration and has been shown to aid recovery in many damage models (Coolican 1997, Barton-Davis 1999, Barton 2002, Mourkioti 2005).

In this study we examined the altered acute recovery response of skeletal muscle when treated with IGF-1, delivered in the PEGylated-fibrin biomatrix, and found increased functionality, improved muscle weight and enhanced regeneration within the first week of recovery.



## **RELATED LITERATURE**

### **ECCENTRIC SKELETAL MUSCLE DAMAGE & REPAIR**

An eccentric muscle contraction involves actively lengthening a muscle. Eccentric muscle damage is responsible for most muscle damage incurred while exercising, can be involved in workplace muscle injuries and underlies the muscle degradation that occurs in muscular dystrophy (Allen 2001). Compared to other skeletal muscle damage models such as crush injury, defect and ischemia/reperfusion, eccentric damage can be less severe, much more common and leads to decreased susceptibility to the same injury if the eccentric bout is repeated in subsequent days. There are three phases of repair that follow the initial, mechanically mediated insult. These phases include: 1) cell membrane lesion and tissue necrosis 2) inflammation and degradation and 3) regeneration. The initial damage leads to an immediate loss of muscle force that peaks around three days post injury and can persist for weeks (Friden and Lieber 2001).

Repeated eccentric contractions result in muscle damage due to mechanical strain. This disrupts the contractile machinery, force bearing components and membrane integrity of an overextended muscle cell and leads to loss of force and increased calcium mediated structural damage (Talbot and Morgan 1996, Zhang 2008, Warren 2001). Eccentric damage is focal in nature. It only occurs where sarcomeres near the membrane

are overextended, and leads to a focal disruption of the membrane (Talbot and Morgan 1996). With thousands sarcomeres composing a muscle fiber, there may be multiple sites of cellular damage, apoptosis of cells and necrosis of tissue.

In the second phase of repair, cytokines released from the damaged tissue call for infiltration of neutrophils, which will peak within several hours of injury. The robust infiltration of neutrophils will be followed by a wave of macrophages. These infiltrate the muscle within 24 hours, peak between days three and five and can persist for 14 days (Beaton 2002). Neutrophils have been shown to mediate muscle tissue degradation through oxidative damage and promote inflammation. They also release chemokines such as hepatocyte growth factor (HGF), interleukin-6, MIF-1 and MCP-1, which help to activate satellite cells (a muscle resident stem cell) and attract macrophages (Toumi 2006). In studies using the eccentric damage model, where the neutrophil response has been ablated, muscle recovery occurred more rapidly, suggesting that their contribution to inflammation and degradation may be in excess (Brickson 2003, Pizza 2005).

The shift from degeneration to regeneration is thought to be controlled by macrophages. Arnold et al. in 2007 showed monocytes (the precursor to macrophages) to infiltrate muscle as pro-inflammatory agents and participate in oxidative damage. Upon phagocytizing the muscle tissue they are phenotypically changed from M1 macrophages into M2 macrophages that will proliferate and promote an anti-inflammatory state and promote regeneration. The growth factors released from the M2 macrophages contribute

to myogenic proliferation, differentiation and fusion of new myoblasts (Arnold 2007).

In summary, the cells of the inflammatory response phagocytose necrotic tissue to clear out debris. The initial damage done by the mechanical strain on susceptible sarcomeres is increased by the activities of these cells, but their phagocytosis and secretion of chemokines is required to move towards the regeneration phase and to beneficially adapt the muscle to eccentric strain (Arnold 2007, Talbot and Morgan 1996).

The satellite cell population is integral to the regeneration of skeletal muscle tissue. They can be activated to proliferate, differentiate into myoblasts and fuse to damaged cells to restore membrane integrity and provide additional nuclei for growth. Research is beginning to elucidate factors that can activate these cells. It has been shown that HGF, nitric oxide (NO) and insulin-like growth factor-1 (IGF-1) can activate satellite cells to start proliferating. After activation, factors such as IGF-1, NO, platelet derived growth factor and fibroblast growth factor guide the satellite cells to differentiate, form myotubes and fuse with myofibers. These chemokines are released from the degraded extracellular matrix and cells such as neutrophils, macrophages and muscle cells (Wozniak 2005).

## **IGF-1 IN REPAIR AND REGENERATION**

Insulin-like growth factor-1 (IGF-1) is a powerful chemical signal in skeletal muscle. Through signaling pathways initiated at the IGF-1 membrane receptor (IGF-1R), it stimulates muscle cell survival and hypertrophy as well as satellite cell proliferation and differentiation (Coolican 1997, Barton-Davis 1999, Barton 2002, Mourkioti 2005). IGF-1 can be produced for systemic release in the liver or locally produced in many tissues including skeletal muscle. Increased paracrine or autocrine release from muscle upon injury can activate the PI3K/AKT pathway. This pathway acts to suppress apoptosis, increase protein synthesis through mTOR and inhibition GSK3 and decrease protein degradation through the phosphorylation of FOXO. It also encourages satellite cell differentiation through MyoD activation and activates the MAPK pathway leading to increased cell proliferation (Coolican 1997).

Though the beneficial signaling pathways of IGF-1 are well defined, its role in functional skeletal muscle repair remains to be determined. Increasing local IGF-1 levels to combat skeletal muscle damage has received increased attention over the last decade. Most of the research into its therapeutic benefits has utilized transgenic mice that overexpress IGF-1 in skeletal muscle tissue. Barton *et. al.* in 2002, tested the effects of overexpressing IGF-1 in the mouse muscular dystrophy (MD) model. This disease results in higher susceptibility to eccentric damage, unceasing degeneration/regeneration cycling and muscle fibrosis as the regenerative capacity of the muscle is exhausted. When compared to untreated MD mice, over-expressors showed less myonecrosis at 3 and 14

months, drastically less fibrosis at 14 months and larger muscle cross sectional areas resulting in 20% more muscle force in the IGF-1 treated MD mouse than the healthy mouse. They hypothesize that these benefits were conferred through IGF-1 activation of the PI3K/AKT and MAPK pathways, which had previously been shown to increase satellite cell activity (Coolican 1997).

Later papers directly confirmed the role of IGF-1 in satellite cell proliferation, differentiation and fusion (Masuro 2003, Hill 2003, Kandalla 2011). Further, based on the timing of up-regulation after injury of certain splice variants of IGF-1, it has been suggested that satellite cell activation is bolstered by this powerful molecule's presence (Hill 2003).

The ability of IGF-1 to lessen the severity of the initial degenerative phase of skeletal muscle repair may also enhance recovery (Barton 2002). In 2007, Pelosi *et.al.* sought to address the ability of IGF-1 to modulate inflammation in a cardiotoxin (a cytotoxic protein derived from snake venom) damage model. Examination of key inflammatory factors such as tumor necrosis factor  $\alpha$  (TNF- $\alpha$ ) and interleukin 1 $\beta$  (IL-1 $\beta$ ) and the infiltration of white blood cells, showed that while IGF-1 overexpression did not the lessen the pro-inflammatory signaling in the early stage of degeneration, it did hasten the transition to the anti-inflammatory/pro-regenerative stage. The IGF-1 over-expressor showed an increased number of centrally nucleated cells and less necrotic cells at five days post injury than the wild type, further indicating a reduced muscle degeneration stage.

The proceeding research suggests that IGF-1 can enhance recovery from muscle injury by potentially decreasing the likelihood of apoptosis, decreasing the magnitude of the inflammatory response and muscle degradation and recruit more satellite cells to become active, proliferate, differentiate and fuse to damaged fibers. Despite these findings relatively few clinical applications of IGF-1 have proceeded to human trials (clinicaltrials.gov). To effectively use IGF-1, direct delivery to a damaged muscle is needed along with a mechanism of stabilizing the molecule and sustaining release.

In novel work by Hammers *et. al.* in 2011, a PEGylated-fibrin biosynthetic matrix was injected 24 hours after ischemia/reperfusion (I/R) of skeletal muscle to provide a sustained delivery of IGF-1 during recovery. This treatment was compared to the injection of bolus IGF-1, a saline solution or the matrix without IGF-1. Significant improvements in muscle force generation at 14 days after injury were found. Further, the sustained delivery of IGF-1, due to the biosynthetic matrix, resulted in a two-fold increase in activation of the PI3K/Akt pathway, when compared to bolus and control treated muscles 4 days after. This work employed a system, comprised of components used in previously FDA approved biomaterials, that delivered a supraphysiological amount of IGF-1 to a localized area and sustained its release over 4 days.

### **PEGYLATED-FIBRIN BIOMATRIX AS A DELIVERY SYSTEM FOR IGF-1**

Having IGF-1 on site during muscle repair can enhance recovery. However, the best way to deliver IGF-1 to the injured area is yet to be determined and will probably

depend on the nature of the injury. IGF-1 delivered in bolus form has limited effects because it diffuses quickly (Hammers 2011). Gene overexpression to load an injured tissue with IGF-1 faces challenges in the clinical setting (Masuro 2004). Using a hydrogel to deliver IGF-1 to the injured muscle allows for local and sustained delivery. The PEGylated-fibrin biomatrix, as used in Hammers 2011, can covalently bind IGF-1 and other growth factors and has been shown to be beneficial to injured muscle tissues. Additionally, IGF-1 delivered in this biosynthetic matrix is simple to administer through an intramuscular injection.

Any biomaterial proposed for use in humans must meet certain standards regarding tissue compatibility and breakdown products. The PEGylated-fibrin biomatrix (PEG-Fib) has been shown to be biocompatible, biodegradable and bioactive. Fibrinogen is a naturally occurring protein monomer involved in clot formation. It forms fibrin in response to thrombin exposure and is popular as a hydrogel due to its innate biocompatibility, bioactivity and biodegradation. It has been shown to bind many growth factors and other naturally occurring proteins (Mosseson 2005). Fibrin composed gels also pose no long term threat to living tissue as they are degraded by native enzymes into harmless byproducts (Bensaid 2003). Poly(ethylene glycol) (PEG) is a synthetic product employed with fibrin to reduce the density of fibrin, modify bioactivity and tailor degradation rates (Zhang 2006, Drinnan 2010). The biocompatibility and biodegradation of PEG-Fib was most recently confirmed by Gonen-Wadmany *et. al.* in 2011. They used a variant of the PEG-Fib hydrogel and showed high smooth muscle cell viability after 14 days of culture in the matrix and matrix susceptibility to enzymatic degradation, as would

occur *in vivo*. Biocompatibility of the PEG-Fib construct has been shown *in vitro* in mesenchymal and embryonic stem cells, smooth muscle cells and cardiac muscle cells and *in vivo* in cardiac and skeletal muscle tissue (Liu 2006, Zhang 2007, Shapira-Schweitzer 2007, Zhang 2008, Hammers 2011).

The PEGylated-Fibrin hydrogel is a safe biomatrix with much therapeutic potential for the delivery of growth factors or cells to injured tissue. In 2006, Zhang *et. al.* seeded PEG-Fib with mesenchymal stem cells (MSCs). They showed an increase in cell proliferation compared to cells in fibrin alone, normal morphology and high cell motility through and out of the matrix. In 2008, research by Zhang *et. al.* used the PEG-Fib construct to treat the myocardial infarction site in mice. PEG-Fib was used to deliver HGF and bone marrow derived mononuclear cells to the damaged cardiac tissue and resulting in decreased apoptosis and increased left ventricular function at four weeks after injury. Drinnan *et. al.* in 2010 showed that PEG-Fib can control the release of more than one growth factor at the site of injury by multiple mechanisms. Specifically, the BB isoform of PDGF, which was entrapped, released to the tissue by diffusion over two days. While transforming growth factor- $\beta$ 1, possessing an innate physical affinity for the fibrin matrix, was held in the biomatrix by affinity and conjugation to the PEG functional groups, and was released from the matrix as it naturally degraded. In addition to being able to attach multiple factors, degradation can be modified by adjusting the PEG:Fib ratio, ultimately allowing the tailored release of any growth factors that can be conjugated to the matrix. These exciting works support PEG-Fib as a safe tool that could



potentially carry a number of beneficial agents to an injury site and release them in an organized manner.

Recently, Hammers *et. al.* delivered IGF-1 covalently bound to PEGylated-Fibrin and demonstrated improved functional recovery in skeletal muscle damaged by I/R when treated 24 hours after injury with IGF-1 conjugated to PEG-Fib (Hammers 2011). This study also established for the first time the release kinetics of IGF-1 from PEG-Fib, showing it to remain in the muscle at physiologically significant levels up to four days post injury while increasing activation of pathways (downstream of IGF-1) involved in protein synthesis, cell survival and myogenesis. Further, with this study, we plan to determine the therapeutic effects of PEG-Fib-IGF-1 in skeletal muscle using an eccentric damage model.

## **SIGNIFICANCE OF STUDY**

As IGF-1 delivery through the PEG-Fib biomatrix has the potential in aiding muscle recovery, this study intends to use the biomatrix to treat eccentric muscle injury. We will evaluate the effectiveness of this novel treatment, which could be easily administered clinically, in aiding recovery from the most common form of muscle injury, which impacts millions of people annually, eccentric damage. The treatment effect will be measured by muscle force recovery, the morphological state of the muscle and magnitude of histological repair at three and seven days after injury.

## METHODS

Male Sprague-Dawley rats (Charles River Laboratories; Wilmington, MA) ages 6-9 months, with an average body weight of  $656.3\text{g} \pm 64.5$ , were utilized in this study. The rats were housed individually, maintained on a 12-hour light cycle and allowed food and water *ad libitum*. Rats were randomly assigned to experimental groups. All animals were obtained from the Animal Resource Center at the University of Texas at Austin and were treated in compliance with the ethical guidelines of the Institutional Animal Care and Use Committee.

### BIOMATRIX PREPARATION & EVALUATION

All hydrogel components were reconstituted in sterile PBS at a pH of 7.8 and prepared sterilely. As previously described in the Hammers *et. al.* 2011, bifunctional SG-PEG-SG (NOF America Corp.) was reacted with human fibrinogen (Hammers *et. al.* used porcine fibrinogen) (Sigma) at a molar ratio of 5:1, respectively. hIGF-1 (Pepprotech) was then conjugated to the PEG-Fib structure to induce a final concentration of 50  $\mu\text{g/ml}$ . Injection into the TA involved a total volume of 0.3 ml. Subsequent to eccentric damage, the vehicle control animals received sterile PBS, while the second control group received the PEG-Fib biomatrix with PBS in place of the IGF-1 volume, and the IGF-1 treated group received IGF-1 conjugated to the PEG-Fib

biomatrix. Gelation was induced by the addition of 25 U/ml hThrombin (Sigma) just prior to injection.

SDS-PAGE followed by western blot analysis was performed as previously described in Hammers 2011. All samples (PEG only, fibrin only, IGF-1 only, PEG-Fib, PEG-IGF-1, Fib-IGF-1 and PEG-Fib-IGF-1) were boiled in 4x Laemmli's sample buffer at a ratio of 3:1. Equal amounts of each sample were load into the wells of the 5% stacking/15% separating polyacrylamide gel along with a protein size latter. Proteins were separated by passing a constant current through the gel. Immediately after sufficient migration of the proteins, they were transferred to a PVDF Millipore membrane and blocked in 5% milk in TBST for 1 hour. The membrane was incubate overnight in a 1:1000 dilution of the hIGF-1-antibody (Pepprotech) in 1% milk-TBST. Resulting protein blots were visualized with ECL detection (Perkin-Elmer) using the Versadoc system (Bio-Rad). Band volume was determined using Quantity One software.

### **INDUCTION OF ECCENTRIC DAMAGE**

Prior to surgery, animals were randomly assigned to one of three experimental groups: PBS, PEG-Fib or PEG-Fib-IGF-1. All surgical procedures were performed in aseptic conditions, using isoflourane anesthesia.

Firstly, the common peroneal nerve was exposed. The ankle was then attached to a servomotor lever system (Aurora Scientific) through an aluminum shoe. The knee was stabilized at a right angle directly above the ankle and body temperature was maintained through a heated mat placed under the rat. Electrodes were inserted next to the exposed nerve. Optimal stimulation voltage was determined by torque measurements applied through the muscle lever and frequency was set to 150 Hz (A-M Systems Isolated Pulse Stimulator, Model 2100). Starting with the ankle at 90°, the dorsiflexor muscles were stimulated for 150 ms then actively stretched to 112% of the *tibialis anterior* (TA) fiber length at a velocity of 1.5 fiber lengths per second. Stimulation was ceased and the ankle was returned to resting length at the same velocity. The total eccentric procedure included three sets of 75 per set, with repetitions occurring every 4 seconds. Five minutes of rest was allowed between each set. After the last set and a 5 minute rest a final force measurement was taken to show equal force loss from the initial force measure. These resulted in about a 67% reduction in force for all animals. After the induction of eccentric damage, the incision to access the nerve was closed and the injection containing 0.3 ml of PBS, PEG-Fib or PEG-Fib-IGF-1 was administered in two injections, evenly infused along the length of the muscle.

### FUNCTIONAL ANALYSIS

Following the 3 or 7 day recovery, an *in situ* measure of the force output (Merritt et al. 2010) of the experimental and contralateral TA was performed. The common peroneal nerve was exposed and the distal tendon of the TA severed and attached to a

servomotor lever system (Aurora Scientific). The distal portion of the TA was separated from connected fascia, while vasculature and nerves remained intact. Muscle temperature was maintained using a heat lamp. The optimal voltage and length were determined in a series of twitch contractions (A-M Systems Isolated Pulse Stimulator, Model 2100). Peak tetanic force (N) was measured at 150 Hz. After each tetany the muscle was allowed to rest for 1.5 minutes. Based on muscle length and weight, physiological cross sectional area (PCSA) was calculated using the formula set forth in Sacks and Roy in 1982, where  $(\text{muscle mass} \times \cos(\text{angle of pennation})) / (\text{muscle density} \times \text{fiber length}) = \text{PCSA}$  and specific tension ( $sP_o$ ) = Force (N) / PCSA ( $\text{cm}^2$ ). Rat *tibialis anterior* muscle density, fiber length and angle of pennation were derived from Eng *et. al.* 2008.

### **HISTOLOGICAL ANALYSIS**

Following functional analysis, both of the rats TA's were excised, measured for resting length and weighed. They were then snap frozen in  $-150^{\circ}\text{C}$  isobutane cooled by liquid nitrogen and stored at  $-80^{\circ}\text{C}$  (Merritt 2010). Transverse sections of  $5\mu\text{m}$  thickness were made from the midbelly of the muscle using a Leica CM1900 cryostat microtome (Leica Microsystems; Wetzlar, Germany). The percentage of fibers with centralized nuclei and a size distribution of fibers within each TA was determined using Haematoxylin & Eosin (H&E).

To determine the dry weight of the muscle and the dry to wet weight ratio, a small piece of the TA was cut from the muscle and immediately weighed, then heated at 80°C until no more weight change was observed (about 4-5 hours), and weighed to determine dry weight.

### **IMAGING AND ANALYSIS**

All H&E sections were imaged with a Nikon Diaphot microscope connected to a Optronix Microfire digital camera. Each muscle section was visualized at 20x magnification, divided into six subsections and two random images were obtained from each. The percentage of fibers with centralized nuclei was determined from a sample of at least 1000 fibers from at least three animals in each experimental group. Using ImageJ (NIH), fiber size distribution ( $\mu\text{m}^2$ ) was also determined from at least 500 fibers from at least three animals in each group. Preliminary analysis indicated that there was no difference in the outcome of size distribution when more than 500 fibers were measured.

### **STATISTICAL ANALYSIS**

Means of all measurements were analyzed utilizing ANOVA with Tukey's post hoc test. Data are represented as mean  $\pm$  standard deviation of the mean. Significance is defined as  $p < 0.05$ .

## RESULTS

### WESTERN BLOT

To verify covalent linkage of IGF-1 to the PEG-Fib biomatrix, a western blot protein analysis was performed with an anti-IGF-1 antibody. The covalent linkage of the growth factor to the biomatrix was confirmed (Figure 1) by the presence of large staining protein complexes in the fibrinogen + PEG + IGF-1 lane. The same demonstration of large PEG-fib complexes with labeled IGF-1 bound to them was demonstrated by Hammers *et. al.* 2011. They went on to show that upon injection of the biomatrix, IGF-1 was released to the muscle in a controlled, sustained fashion.

### FUNCTIONAL

Three and seven days after eccentric damaged was induced and the treatment injection of PBS, PEG-Fib (PF) or PEG-Fib-IGF-1 (PFI) administered, *in situ* maximal isometric tetanic force ( $P_o$ ) was measured in the damaged muscle and compared to the contralateral control muscle to determine the force deficits within each group (Figure 2). Table 1 lists maximal tetanic force ( $P_o$ ) and specific tension ( $sP_o$ ), while deficits of these compared to contralateral controls can be found in Table 2. In the 3 day recovery group, the PFI treated muscles generated significantly greater force as a percentage of the contralateral control than the PBS treated muscle ( $61.3\% \pm 8$  vs.  $37.3\% \pm 13.3$ ;  $p = 0.003$ ), while the PF muscle was not found to be different than either ( $51.6\% \pm 7.4$ ). After 7 days



of recovery, the PBS muscles had improved significantly compared to the 3 day force ( $68.3\% \pm 3.9$ ;  $p = 0.021$ ), while neither PF or PFI had improved significantly compared to their 3 day forces deficits ( $58.2\% \pm 17.7$ ,  $71.6\% \pm 6.1$ , respectively). The force deficits in the 7 day recovery groups were not found to be significantly different. This suggests that the presence of IGF-1 imparted an appreciable beneficial effect within the first three days of recovery, but not between day three and seven.

### **MORPHOLOGICAL**

After force measurements were performed, then damaged and contralateral control muscles were assessed for weight and length, and snap-frozen for histological analysis. Table 2 lists wet weights and physiological cross sectional areas of all damaged muscle, along deficits of these parameters compared to contralateral controls. As shown in Table 2 and Figure 3, the 3 day recovery groups muscles weighed more than their contralateral controls (PBS3-  $108.6\% \pm 5.4$ , PF3-  $105.6\% \pm 10.6$  and PFI3-  $115.2\% \pm 13.3$ ). At 7 days post injury, the only group to maintain a positive weight ratio compared to the contralateral control was PFI ( $105.3\% \pm 4.4$ ), which was also significantly higher than the weight deficits seen in the PBS and PF muscles (PBS7-  $88.3\% \pm 3.4$ , PF7-  $83.1\% \pm 9$ , significantly lower than PFI7 with  $p$  values of 0.021 and 0.002, respectively). This shows that the presence of IGF-1 in early recovery helps to attenuate the negative swing in

muscle weight, suggestive of a loss of proteins, otherwise seen with eccentric damage after seven days of recovery.

The ratio of dry to wet weight of a muscle has been used to evaluate the amount of edema, or fluid gain, after injury (Judge 2003). No significant difference was seen between control tissues and treatment tissues in any treatment group (Table 1). This suggests that there was no significant increase in edema within the first week of recovery from the eccentric damaged we induced.

### **HISTOLOGICAL**

After muscle damage, muscle fibers begin repair within a couple of days. A sign of this process is the migration of the nuclei from the periphery of the fiber to the center, as seen in Figures 7 and 8 (Faulkner 1989, Joya 2004). Upon analysis of the percentage of centrally nucleated fibers (CNFs), we found that PFI treated muscle had an earlier and greater increase in CNFs (Figure 9). At 3 days, PBS and PF fibers showed a slight increase above control with  $1.75\% \pm 1$  and  $1.68\% \pm 1.2$  of their fibers displaying centrally located nuclei. However, PFI muscles had  $5.57\% \pm 0.6$  fibers with central nuclei. This is significantly higher than control, PBS and PF muscles ( $p = 0.002$ ,  $p = 0.014$  and  $0.03$ , respectively). Seven days after injury, PFI muscles had  $13.22\% \pm 3.4$  CNFs, which was still significantly greater than PBS ( $9.63\% \pm 2$ ;  $p = 0.025$ ) and PF ( $8.79\% \pm 1.4$ ;  $p = 0.009$ ).

A fiber size distribution can be used to quantify the presence of swollen fibers soon after damage and small, regenerating fibers indicative of regeneration (Faulkner

1989). In Figures 5 and 6, fiber size distributions are shown by treatment type for the 3 and 7 day post injury muscles with the control muscle distribution in gray. Control muscle displayed a normal distribution with a mean fiber size of  $3359.45\mu\text{m}^2 \pm 1606.9$  (Figure 4, 5 and 6). All 3 day recovery groups showed a higher mean fiber size (PBS3-  $3553.96\mu\text{m}^2 \pm 1692.2$ , PF3-  $3906.67\mu\text{m}^2 \pm 2238.9$  and PFI3-  $3956.96\mu\text{m}^2 \pm 2311.9$ ). At 7 days after injury, the PBS and PF treated muscles had a smaller mean fiber size than the control tissue and their 3 day treatment pair ( $2877.16\mu\text{m}^2 \pm 1807.3$  and  $2508.25\mu\text{m}^2 \pm 1922.1$ ), while the mean fibers size of the PFI muscles, maintained a mean fiber size similar to control tissue, though they had an increase in small, regenerating fibers.

## FIGURES

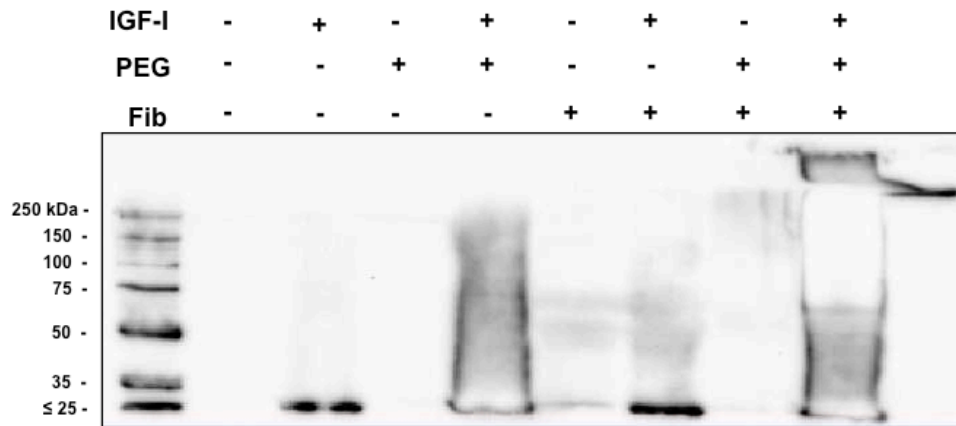


Figure 1. Western blotting with anti-IGF-1 antibody (dark stain) verifies covalent linkage of IGF-1 on PEG-Fib biomatrix. The largest complexes were found in the PEG + Fib + IGF-1 lane with the protein sizes above 250 kDa according to the protein size ladder in the first lane.

	PBS 3	PBS 7	PF 3	PF 7	PFI 3	PFI 7	Control
Dry:wet weight (%)	19.6 (1.81)	21.8 (1.98)	20.06 (1.09)	20.79 (1.57)	19.05 (2.55)	20.59 (0.30)	21.9 (2.1)

Table 1. Dry weight of TA expressed as a percentage of wet weight. No significance differences were. Trend observed in dry weight percentage increasing from 3 to 7 days of recovery.

	Control	PBS 3	PF 3	PFI 3	PBS 7	PF 7	PFI 7
Body Weight (g)		618.4 (72.5)	662.8 (41.1)	694.3 (64.5)	660.7 (68.4)	659.2 (60.9)	658.0 (63.3)
Muscle Weight (g)	1.28 (0.12)	1.3 (0.14)	1.34 (0.06)	1.45 (0.2)	1.13 (0.12)	1.05 <sup>a,c</sup> (0.17)	1.37 (0.15)
PCSA (cm <sup>2</sup> )	0.69 (0.06)	0.71 (0.08)	0.7 (0.04)	0.8 <sup>a</sup> (0.11)	0.6 <sup>a,c</sup> (0.06)	0.58 <sup>a,c</sup> (0.06)	0.74 (0.06)
P <sub>o</sub> (N)	18.5 (2.0)	6.93 <sup>a,b,c</sup> (2.8)	9.9 <sup>a</sup> (1.2)	11.37 <sup>a</sup> (2.8)	12.11 <sup>a,b</sup> (1.3)	10.7 <sup>a</sup> (3.4)	13.38 <sup>a</sup> (1.4)
sP <sub>o</sub> (N/g/cm <sup>2</sup> )	26.8 (2.2)	9.8 <sup>a,b</sup> (3.93)	14.14 <sup>a</sup> (1.69)	14.25 <sup>a</sup> (3.1)	20.34 <sup>a,b</sup> (1.9)	18.14 <sup>a</sup> (4.56)	18.13 <sup>a</sup> (1.86)

Table 2. Morphometric and functional data expressed as mean (SD). Physiological cross sectional area (PCSA), Maximal isometric tetanic force (P<sub>o</sub>), Specific tension (sP<sub>o</sub>). Control values were pooled from all control legs. a significantly different from control, b significantly different from treatment pair, c significantly different from time-matched PFI.

	PBS 3	PF 3	PFI 3	PBS 7	PF 7	PFI 7
Muscle Weight (%)	108.6 <sup>b,c</sup> (5.4)	105.6 (10.6)	115.2 (13.3)	88.3 <sup>b</sup> (3.4)	83.1 (9.0)	105.3 (4.4)
PCSA (%)	107.4 (8.0)	101.7 <sup>c</sup> (6.1)	114.2 (14.4)	88.3 <sup>c</sup> (3.3)	81.2 <sup>c</sup> (5.1)	105.3 (4.4)
P <sub>o</sub> Deficit (%)	37.3 <sup>b,c</sup> (13.3)	51.6 (7.4)	61.3 (8.0)	68.3 <sup>b</sup> (3.9)	58.2 (17.7)	71.6 (6.1)
sP <sub>o</sub> (%)	35.1 (13.1)	50.5 (4.9)	52.4 (10.8)	77.5 (4.7)	71.1 (19.3)	68.3 (8.7)

Table 3. Morphometric and functional data expressed as a percentage of the contralateral control. a significantly different from control, b significantly different from treatment pair, c significantly different from time-matched PFI.

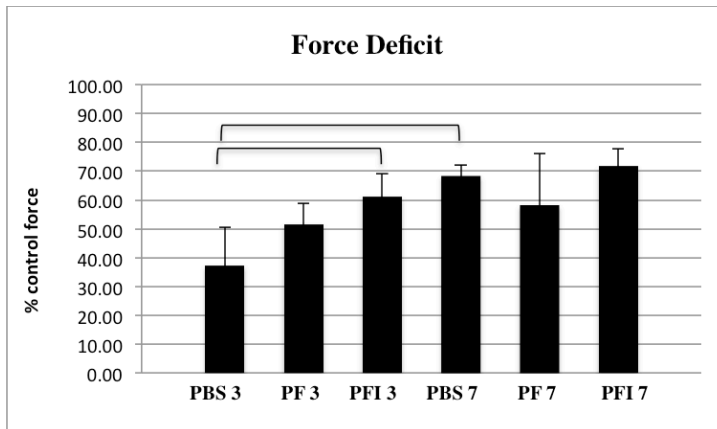


Figure 2. *In situ* measure of maximal force generation (N) of recovering muscle, expressed as percent of contralateral control force. Brackets indicate p-values < 0.01.

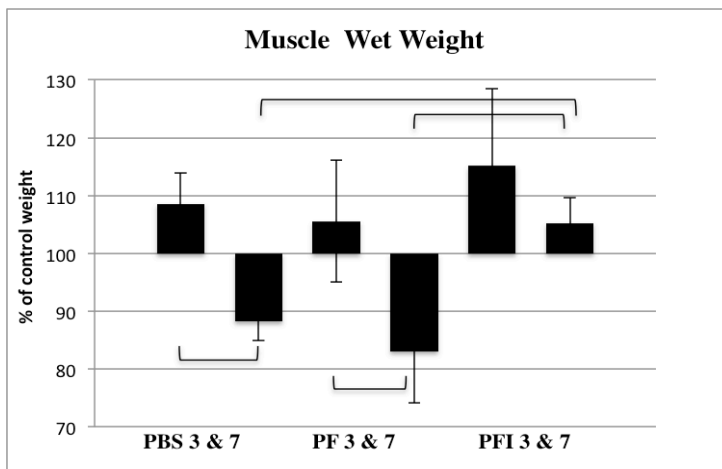


Figure 3. Weight change after injury, expressed as percentage of contralateral control weight. Brackets indicate p-values < 0.005.

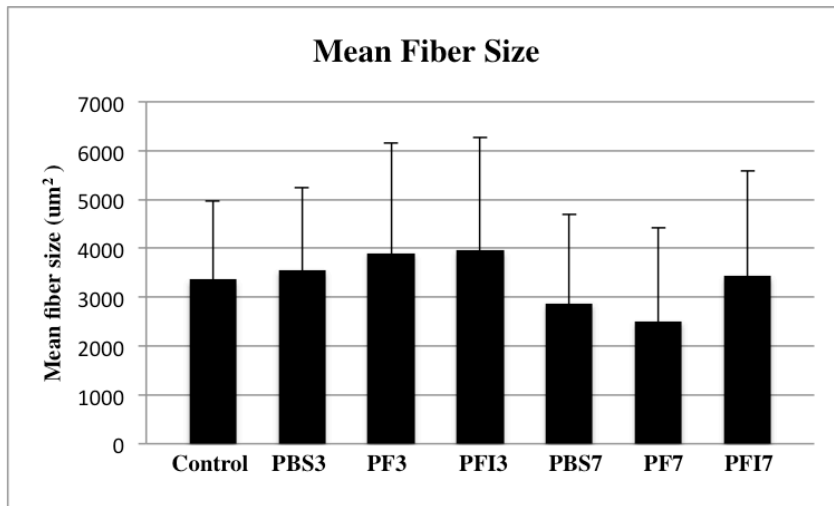


Figure 4. Mean fiber size of control and treatment groups ( $\mu\text{m}^2$ ) with SD.

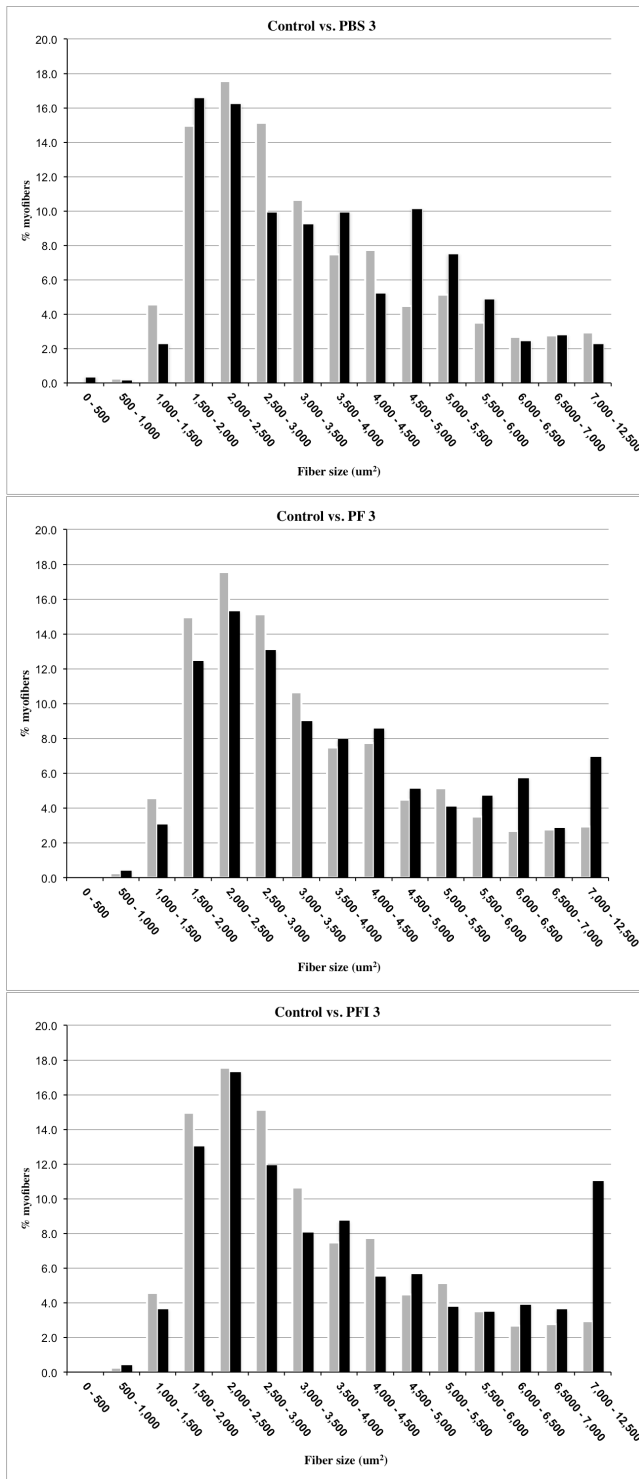


Figure 5. Myofiber size distribution at 3 days post-injury. Control fiber sizes seen in gray, experimental fiber sizes in black.



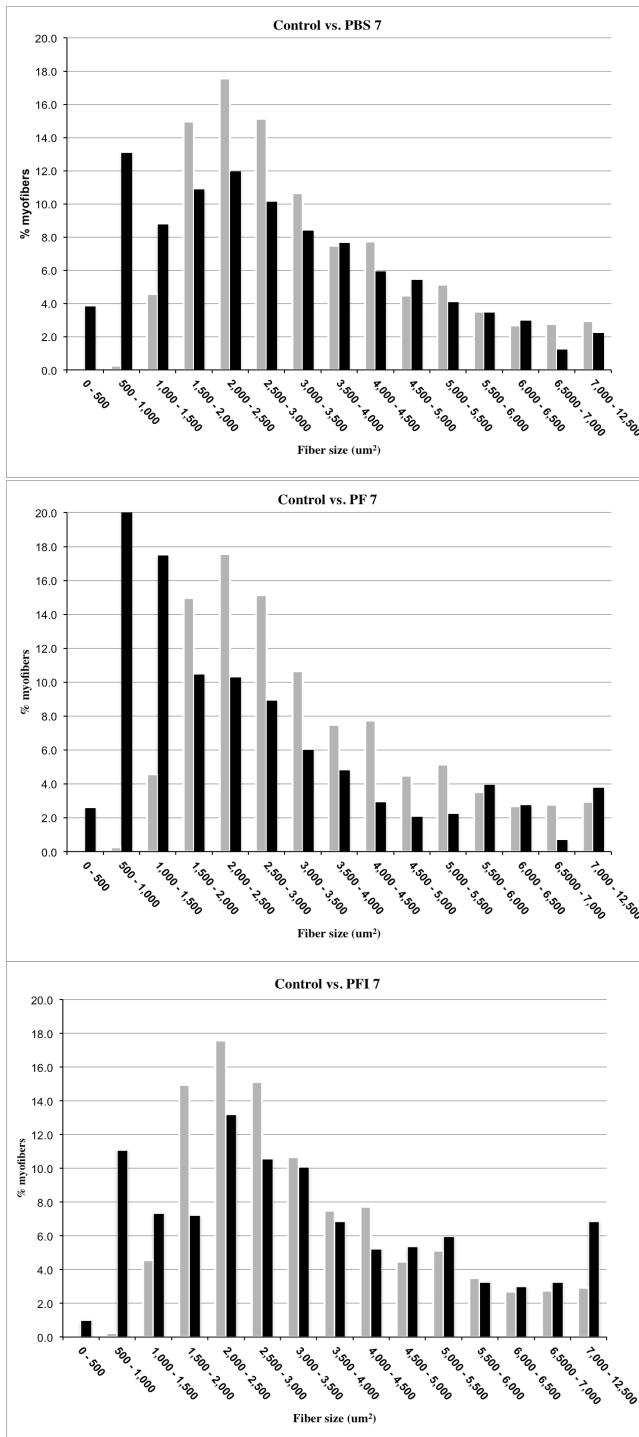


Figure 6. Myofiber size distribution 7 days post injury. Control fiber sizes seen in gray, experimental fiber sizes in black.

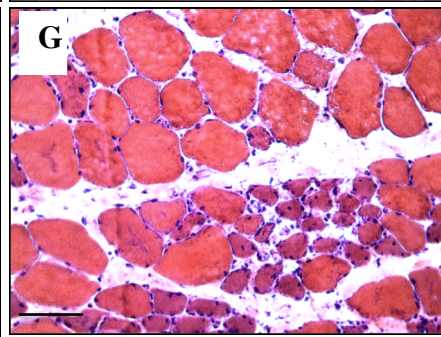
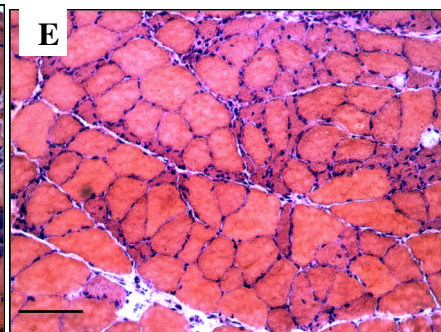
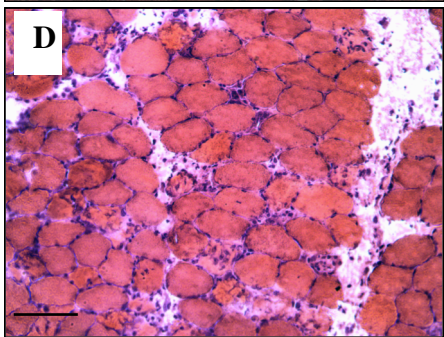
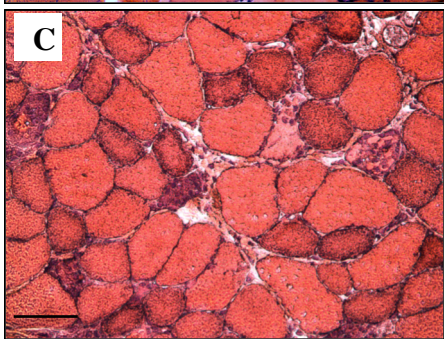
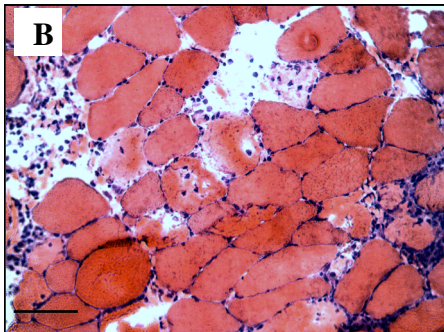
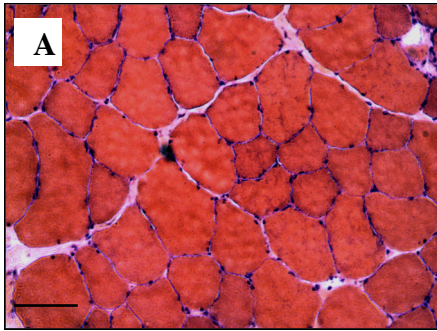


Figure 7. Histological evaluation of fibers with H&E staining. (A) represents uninjured tissue, (B), (C) and (D) represent tissue 3 days post injury, (E), (F) and (G) represent tissue 7 days post-injury. (B) and (E) are PBS treated, (C) and (F) are PF treated, and (D) and (G) were treated with PFI. Viewed with 20x objective power. Scale bar = 100 $\mu$ m.

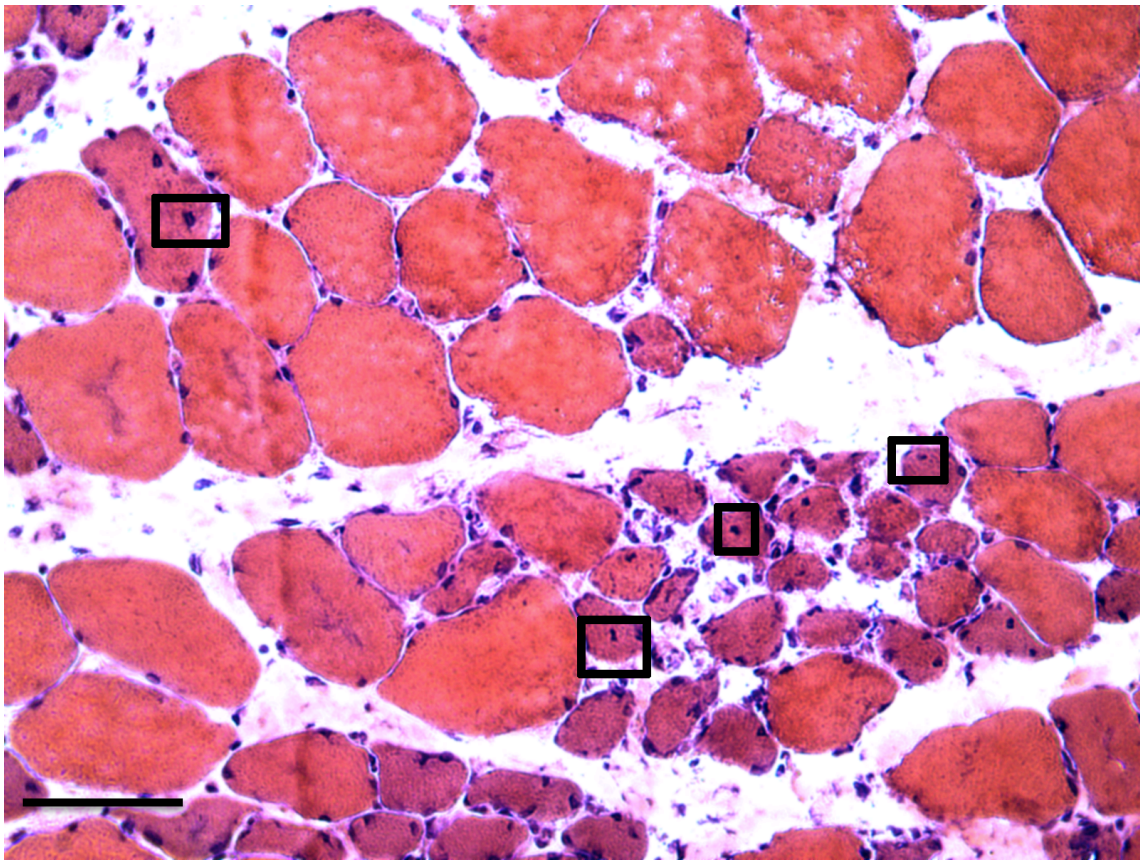


Figure 8. Example of centrally nucleated fibers (black rectangles) from the PFI 7 muscle seen in Figure 7. Viewed with 20x objective power. Scale bar = 100  $\mu$ m.

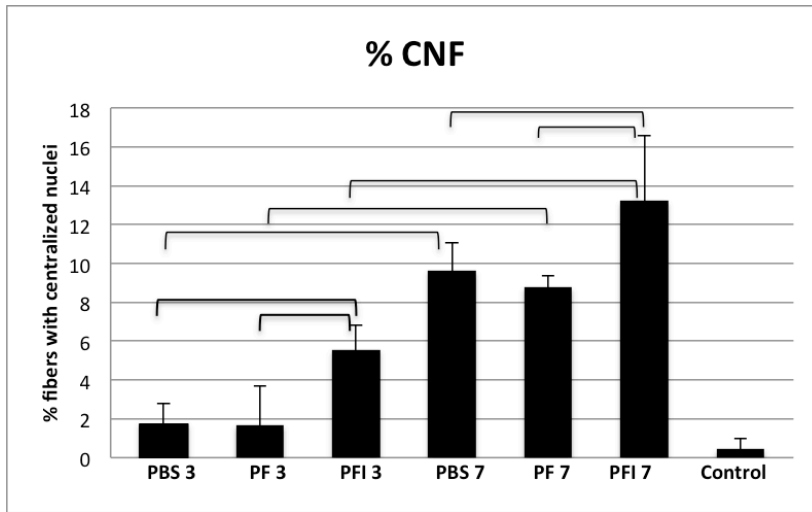


Figure 9. H&E staining was used to determine the percentage of the total fibers with centralized nuclei. All groups were significantly above control value. All treatment pairs had p-values < 0.001. Brackets within recovery time groups indicate p-values < 0.05.

## DISCUSSION

The purpose of this study was to evaluate the acute treatment effect of IGF-1, delivered in a PEGylated-fibrin biomatrix, in a muscle damaged by eccentric lengthening contractions. To our knowledge this treatment has not been studied in the eccentric damage model or in skeletal muscle at acute time-points. The administration of the IGF-1 treatment after 225 eccentric contractions attenuated the loss in force seen 3 days after injury, it prevented the negative weight swing seen between days 3 and 7 of recovery, it helped maintain a more normal fiber size and resulted in an earlier and greater amount of centrally nucleated fibers, signifying better repair/regeneration.

Hammers 2011 used the same PEG-Fib biomatrix with a lower concentration of IGF-1 and treatment volume and reported a sustained release of IGF-1 after 3 days. Despite a majority being release in 24 hours of delivery, a physiologically relevant amount of IGF-1 remained in the matrix at 96 hours after polymerization. In this study, we were able to deliver a total of 7.5  $\mu\text{g}$  of IGF-1 to the damaged muscle (average weight of 1.28g) in a controlled release fashion and, like Hammers 2011, report significant improvements in recovery.

By our damaged muscles with IGF-1 within one hour of injury, this potent molecule was available to increase cell survival and protein synthesis. We believe this beneficial role of IGF-1 was demonstrated in the smaller force deficit seen at 3 days compared to the PBS group. We do know, from Hammers *et. al.* in 2011, where the treatment was delivered 24 hours after I/R injury, that the IGF-1 released from the

biomatrix resulted in a  $\approx 2$ -fold elevation in AKT and mTOR phosphorylation 4 days after ischemia/reperfusion injury. Activation of the AKT/PI3K pathway promotes cell survival and increases muscle protein synthesis.

The normal response to skeletal muscle damage involves a rise in muscle wet weight seen 3 days after injury, which is thought to be a sign of inflammation and possibly edema. This is followed by a severe decrease in wet weight, below control values, thought to be due to the loss of damaged cellular and protein content, which is detectable after major inflammation ceases. Though our dry to wet weight ratios did not suggest significant fluid gain (edema) at day 3, muscle wet weights were still significantly increased from control. Edema occurs due to increased capillary permeability, usually associated with oxidative damage in skeletal muscle (Judge 2003). Significant edema may not have occurred because oxidative damage does not play a role in the initial eccentric injury, and eccentric damage is less severe than other injury models where significant edema is found (Allen 2001). Further, we found that the sustained release of IGF-1 did attenuate the drastic loss in muscle weight seen between day 3 and 7 in the PBS and PF groups. We believe that the aforementioned activation of the AKT/PI3K pro-cell survival pathway conferred this effect by lessening the total degradation of muscle content (Kooijman 2002).

In agreement with the finding of healthier muscle weights in the PFI7 group, mean fiber area of this group was nearest the control fiber area, while the PBS7 and PF7 muscles were found to be smaller. The fiber size distribution of the PFI7 muscle also



showed less of a leftward shift and maintenance of larger fibers. These data suggest morphological benefits of the IGF-1 treatment within the first week of recovery.

Lastly, at 3 days and 7 days after injury the IGF-1 treated muscles contained significantly more centrally nucleated fibers than the other two treatment groups. Central nucleation is a sign of regeneration. As mentioned above, recovery from eccentric damage occurs in three step-wise, but overlapping phases. The appearance of more central nuclei earlier in the recovery process suggests that the delivery of IGF-1 soon after injury lessened the magnitude of cell death and degradation, allowing a more rapid transition to the regeneration phase. Histologically, less necrosis was observed and more central nuclei in new myotubes were seen. Endogenous IGF-1 expression is known to increase rapidly within days of injury and has been shown to encourage satellite cell proliferation and differentiation (Hill 2003, Masuro 2003). We believe to supra-physiological level of IGF-1 that we delivered accelerated and increased this process.

In conclusion, the PEGylated-Fibrin biomatrix offers a novel delivery system for the potent IGF-1 molecule for treatment of eccentric muscle damage. The early and sustained delivery resulted in improvements of the function, weight, and fiber size in acute recovery and sooner progression to regeneration. Further studies are warranted to investigate the performance of the biomatrix in other injury models with other possible beneficial molecules that can be delivered.

## **APPENDICES**

### **A: BIOMATRIX PREPARATION**

(All done in sterile flow hood with sterile practice, using pH 7.8 PBS)

#### Protocol:

- pH sterile PBS to 7.8 by adding NaOH, dropwise, then autoclave
- Reconstitute hFib in PBS pH 7.8, to a concentration of 80 mg/ml in a 1 ml tube, vortex and incubate in 37° C water bath for 1 hour
- Filter fibrinogen solution using a 3 ml syringe and Millex 0.22µm syringe filter
- Reconstitute PEG to a 40 mg/ml concentration in PBS
- Prepare IGF-1 solution to the concentration of 100 µg/ml
- For a 0.3 ml injection, add 50 µl of the hFib solution, 50 µl of the PEG solution, and 100 µl of the IGF-1 solution and allow to incubate at room temperature for 45 minutes
- Just prior to injecting the hydrogel, thaw hThrombin at a 25U/ml concentration and draw into the syringe 0.15 ml, next draw up 0.15 ml of the PEG-Fib-IGF-1 hydrogel and invert to mix



## **B: BIOMATRIX PROTEIN ANALYSIS**

(Based on procedure by David Hammers)

### Sample Preparation

- Label tubes for reaction: PBS, IGF-1, PEG, Fib, IGF-1 PEG, IGF-1 Fib, PEG Fib, IGF-1 PEG Fib
  - add 20  $\mu$ l of IGF-1 to IGF-1 tubes
  - add 10  $\mu$ l of PEG to PEG tubes
  - add 10  $\mu$ l of Fib to Fib tubes
  - add PBS pH 7.8 to bring to a 80  $\mu$ l volume
- Vortex and allow sample to incubate for 1 hour at 37° C
- Thaw Lammeli's 4x sample buffer and half the concentration with DI water
- Add 50  $\mu$ l to each sample
- Boil for 5 min

### SDS-Polyacrylamide Gel Electrophoresis (SDS-PAGE)

- Gather 15 mL conical tubes, glass slides, and all gel casting equipment
- Wipe both sides of all glass slide with methanol
- Assemble gel casting apparatus
- Mix both the 15% separating and the 5% stacking gels simultaneously in their respective tubes
- Add APS and TEMED to separating gel

- Vortex briefly and pipette into gel casting plates until it is ~2 inches from top of short plate
- Carefully add butanol over poured separating gel to ensure a smooth surface
- Allow separating gel to polymerize
- Pour out butanol and rinse thoroughly with dH<sub>2</sub>O
- Absorb excess H<sub>2</sub>O with KimWipe.
- Add APS and TEMED to stacking gel and pour over separating gel
- Place comb over top and make sure no air bubbles are trapped
- Allow stacking gel to polymerize
- Remove from casting stand and place in electrophoresis module
- Fill inner space with 1X Running buffer and remove combs
- Place the sample loading guide over inner space and load 5 µl of protein marker and load appropriate amounts of prepared sample into correct lanes.
- Remove sample loading guide, fill outer space with 1X Running buffer until 1/3 to 1/2 the height of the gel
- Cover with electrophoresis module cover
- Turn ON power supply and set to constant current to 50 mA, 200 V, and 200 W
- Run until separation is achieved

#### Transfer to PDVF Membrane

- Pour an appropriate amount of Anode I solution into a weigh boat.

- Remove gel from electrophoresis module and carefully remove short plate.
- Cut a piece of PDVF membrane the size of the gel
- Place this into pure methanol, then move to another weight boat containing Anode I solution and allow to equilibrate for 5 minutes
- Cut 2 pieces of extra-thick blotting paper that corresponds in size to the membrane
- Soak 1 of these in Anode II solution
- Open transfer cell and gently place Anode II solution-soaked blotting paper to electrode, making sure to remove air bubbles
- Remove membrane from Anode I solution and place on top of blotting paper
- Place soaked gel over membrane
- Soak other piece of blotting paper in Cathode solution, remove and place over gel
- Replace transfer cell cover and turn ON power supply
- Set to 300 mA constant current, 25 V, and 200 W

### Immunoblotting

- Prepare 25 mL of 5% milk in TBST
- Pour milk into plastic shaking dish and spin down
- Remove membrane from transfer cell and place in milk
- Rotate at room temperature for at least 1 hour
- Prepare 5 mL of 1% milk-TBST and transfer to a properly labeled 15 mL conical tube

- Add appropriate amount of primary antibody to achieve 1:1000 dilution
- Pour milk out of shaker and add a small amount of TBST to rinse milk off of membrane
- Remove membrane from shaker and curve to fit into the tube containing the prepared primary antibody solution and allow to rotate overnight at 4° C
- Add ~15 mL of TBST to a plastic shaker, and remove membrane from 15 mL conical tube to place in shaker
- Rotate at room temperature for 15 minutes. Perform 3 washes total.
- Prepare 10 mL of 5% milk-TBST with secondary antibody to achieve a 1:2000 dilution
- Rotate at room temperature for at least 1 hour
- Dump out secondary antibody solution, rinse with TBST, and perform 5 5-minute washes with TBST.

#### Immunoblot Developing

- Prepare ECL solution by adding 1 mL of each reagent together in a 15 mL conical tube
- After the 5<sup>th</sup> TBST wash, rinse membrane briefly with dH<sub>2</sub>O and transfer to flat dish
- Pipette ECL solution on to membrane, do not disturb the surface tension that holds the solution over the membrane
- Incubate for 5 minutes

- Blot off excess ECL solution on KimWipes and place membrane on clear sheets
- Turn on equipment, remove lens cap and place membrane on tray
- Open Quantity One and turn on EpiWhite light and click Live Focus
- Adjust membrane position and focus manually if needed
- Once aligned, turn off EpiWhite light and click freeze
- Use Manual Acquire to test a 15 sec exposure, then Live Acquire for 8-15 min at 20 second increments
- Edit best picture with cropping tool bar, rotate to straighten, then save
- Under Imaging, subtract background and save
- Download to Quantity one to create volume boxes
- Set volume report options to: volume, adjust volume, density, local subtraction
- Export in excel format and use adjust volume in excel

### **C: INDUCTION OF ECCENTRIC DAMAGE**

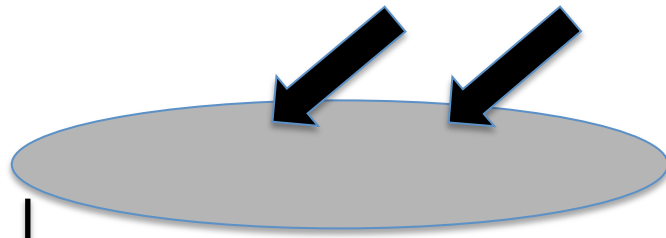
(Procedure performed in sterile conditions, animal's depth of anesthesia was checked every 15 minutes and recorded)

#### Protocol:

- After the animal is weighed, place it in the anesthesia chamber containing 2.5 % isoflurane (animal is fully anesthetized when they do not respond to a toe pinch or eye touch)
- Administer the weight adjusted dose of the analgesic (Rimadyl), 5 mg/kg, subcutaneously, just below the xiphoid process
- Shave the experimental leg, disinfect the skin in the surgical area with iodine and place the animal on the heating pad to maintain body temperature
- Make an incision through the skin and *vastus lateralis*, parallel to the femur, starting just above and behind the head of the fibula
- Separate the peroneal nerve from the surrounding fascia and slip the insulated electrodes under the nerve
- Transfer the animal to the eccentric platform and, with the animal laying on his side, securely attach the foot to the aluminum boot
- Stabilize the behind the hip and in front of the knee to insure no movement at the knee joint during the protocol

- Attach the electrode to the Isolated Pulse Stimulator and find the initial maximal force of tetany ( $P_o$ ) by adjusting optimizing voltage, while keeping frequency at 150 Hz
- Once  $P_o$  is found, begin the eccentric regime which involves a 150 ms isometric contraction, immediately followed by a  $35^\circ$  extension (eccentric contraction) at the ankle joint at a velocity of 1.5 fiber lengths per second, stimulation stops after the eccentric contraction and the ankle is returned at the same velocity to  $90^\circ$ , allowed to rest for the remainder of 4 seconds
- After 3 sets of 75 contraction with 5 minutes rest between each set, take a final isometric force measurement after the last 5 minute rest  
(Force measurements after each set showed a similar decline in force between muscle, usually around a third of the original force. This demonstrates similar excretions by all muscles.)
- Remove the animal from the platform and remove the electrodes from the incision
- Suture the muscle and skin incision closed with 5-0 prolene sutures in a interrupted pattern
- Administer the assigned treatment in 2 injections sites in the mid-top and mid-bottom of the TA, in manner where the needle tip is placed deep into the muscle, towards the knee at an oblique angle, then release gel as withdrawn

Diagram of TA muscle with arrows as needle.



(Superior end, ventral aspect of TA muscle)

- Monitor and allow animal to recover for 3 or 7 days



## **D: FORCE MEASUREMENT AND TISSUE HARVEST**

### Protocol:

- Weigh animal, anesthetize and shave as mentioned above
- Isolate the peroneal nerve as mentioned above
- Remove the skin and fascia covering the dorsiflexor muscle cavity, isolate the TA, and sever the distal tendons of the TA, *extensor digitorum longus* and *extensor hallucis longus*
- Transfer the animal to the force platform and secure the knee joint to the platform
- Attach the distal tendon of the TA to the servomotor lever arm and position the electrodes on the peroneal nerve
- Find optimal voltage and muscle length through a series of twitch contractions
- Measure maximal tetanic force of the TA at a frequency of 150 Hz, allowing 1.5 minutes rest between each tetany
- After the force measurement is complete for both legs, excise the TA's and euthanize the animal by exsanguination
- Record length and weight of TA's
- Place the muscle at resting length on a wooden craft stick lined with OCT mixed with Tragacanth (Sigma) powder and cover muscle with OCT (Tissue Tek)
- Snap freeze the muscle in isopentane cooled by liquid nitrogen, cover in foil and store in -80° freezer

## **E: HISTOLOGICAL ANALYSIS**

### Protocol:

- For histological analysis 5  $\mu\text{m}$  thick sections were mounted on microscope slides and allowed to dry for 30 minutes
- With 5 slides per jar, apply Harris Hematoxylin solution (stains nuclei blue) for 5 minutes
- Then rinse slides in tap water until clear
- Apply Eosin stain (stains proteins pink) for 2 minutes
- Tap water rinse till clear, followed by rinses in 70%, then 100% Ethanol for several seconds each
- Rinse with Xylene in hood for several seconds
- Wash with 70% Ethanol and allow sections to dry
- Permount was then used to mount a coverslip
- One set, involving 12 images, was made for each muscle
- Images were opened and analyzed using ImageJ, an NIH, user generated image analysis software
- To determine the fiber size distribution a sample of 500-1000 fibers was measured using the ROI ImageJ plugin which involves converting area of a fiber in pixels to  $\mu\text{m}^2$
- To determine the percentage of the fibers with centralized nuclei a sample of at least 1000 fibers were counted and designated as having centralized nuclei or not.

# **F: RAW MORPHOMETRIC AND FUNCTIONAL DATA**

Force	Body weight(g)	Damaged muscle(N)	Contralateral control (N)	Po deficit
Ecc 130	556	2.7	13.6	19.85
Ecc 230	591	3.6	18.5	19.46
Ecc 330	575	9.1	20.66	44.05
Ecc 430	644	8.44	18.6	45.38
Ecc 530	640	7.6	15.4	49.35
Ecc 630	730	4.86	18.3	26.56
Ecc 730	696	9.7	23.3	41.63
Ecc 830	515	9.41	18	52.28
Ecc 270	636	11.01	15.5	71.03
Ecc 370	623	12.4	17.53	70.74
Ecc 470	612	13	18.88	68.86
Ecc 570	642	10.68	16.05	66.54
Ecc 670	797	14	19.58	71.50
Ecc 770	654	11.54	18.8	61.38
Ecc 131	694	9.66	18.93	51.03
Ecc 231	642	10.33	18.61	55.51
Ecc 431	700	8.38	20.24	41.40
Ecc 531	615	11.210	19.22	58.32
Ecc 171	764	10.22	18.81	54.33
Ecc 271	633	8.7	17.38	50.06
Ecc 371	646	6.45	18.5	34.86
Ecc 571	606	13	17.39	74.76
Ecc 671	647	15.07	19.55	77.08
Ecc 232	767	10.4	19.48	53.39
Ecc 332	776	9.24	16.98	54.42
Ecc 432	687	12.06	20.11	59.97
Ecc 532	672	15.93	21.07	75.61
Ecc 632	616	12.38	19.65	63.00
Ecc 732	648	8.2	17.11	61.28
Ecc 172	734	15.42	23.3	66.18
Ecc 272	572	13.8	17	81.18
Ecc 472	654	13.21	19.12	69.09
Ecc 572	702	11.6	17.17	67.56
Ecc 672	628	12.85	17.34	74.11

Eccentric leg				Control leg		
	Muscle weight	PCSA (cm <sup>2</sup> )	sPo (N/g/cm <sup>2</sup> )	Muscle weight	PCSA	sPo
Ecc 130	1.19	0.643	4.20	1.11	0.599	22.69
Ecc 230	1.27	0.686	5.25	1.18	0.637	29.04
Ecc 330	1.08	0.583	15.61	1.07	0.642	32.18
Ecc 430	1.34	0.724	11.67	1.2	0.648	28.71
Ecc 530	1.27	0.686	11.08	1.23	0.664	23.19
Ecc 630	1.32	0.713	6.82	1.14	0.616	29.73
Ecc 730	1.55	0.837	11.59	1.45	0.783	29.76
Ecc 830	1.34	0.775	12.14	1.16	0.671	26.82
Ecc 270	1.06	0.572	19.24	1.18	0.637	24.33
Ecc 370	1.26	0.680	18.23	1.37	0.740	23.70
Ecc 470	1.04	0.562	23.15	1.25	0.675	27.97
Ecc 570	1.05	0.567	18.84	1.15	0.621	25.85
Ecc 670	1.3	0.658	21.27	1.49	0.754	25.96
Ecc 770	1.07	0.542	21.31	1.24	0.628	29.95
Ecc 131	1.28	0.691	13.98	1.3	0.702	26.97
Ecc 231	1.4	0.658	15.70	1.18	0.637	29.21
Ecc 431	1.31	0.707	11.85	1.37	0.740	27.36
Ecc 531	1.38	0.745	15.04	1.26	0.680	28.25
Ecc 171	1.13	0.610	16.75	1.39	0.751	25.06
Ecc 271	0.823	0.497	17.51	1.04	0.602	28.89
Ecc 371	0.91	0.546	11.81	1.28	0.740	24.98
Ecc 571	1.17	0.632	20.58	1.24	0.717	24.24
Ecc 671	1.2	0.627	24.03	1.345	0.778	25.13
Ecc 232	1.41	0.737	14.12	1.26	0.680	28.63
Ecc 332	1.55	0.837	11.04	1.14	0.613	27.71
Ecc 432	1.8	0.972	12.41	1.44	0.778	25.86
Ecc 532	1.37	0.854	18.66	1.3	0.752	28.02
Ecc 632	1.28	0.715	17.32	1.27	0.735	26.75
Ecc 732	1.27	0.686	11.96	1.14	0.658	26.01
Ecc 172	1.54	0.805	19.16	1.43	0.747	31.18
Ecc 272	1.2	0.694	19.88	1.22	0.706	24.09
Ecc 472	1.44	0.778	16.99	1.38	0.745	25.66
Ecc 572	1.44	0.752	15.42	1.31	0.685	25.08
Ecc 672	1.24	0.670	19.19	1.17	0.632	27.45

	sPo deficit	Muscle weight deficit
Ecc 130	18.52	107.21
Ecc 230	18.08	107.63
Ecc 330	48.49	100.93
Ecc 430	40.64	111.67
Ecc 530	47.80	103.25
Ecc 630	22.94	115.79
Ecc 730	38.95	106.90
Ecc 830	45.26	115.52
Ecc 270	79.07	89.83
Ecc 370	76.91	91.97
Ecc 470	82.76	83.20
Ecc 570	72.88	91.30
Ecc 670	81.95	87.25
Ecc 770	71.14	86.29
Ecc 131	51.83	98.46
Ecc 231	53.75	118.64
Ecc 431	43.30	95.62
Ecc 531	53.25	109.52
Ecc 171	66.83	81.29
Ecc 271	60.63	79.62
Ecc 371	47.29	71.09
Ecc 571	84.89	94.35
Ecc 671	95.66	89.22
Ecc 232	49.30	111.90
Ecc 332	39.85	136.56
Ecc 432	47.98	125.00
Ecc 532	66.62	105.38
Ecc 632	64.74	100.79
Ecc 732	45.97	111.70
Ecc 172	61.45	107.69
Ecc 272	82.53	98.36
Ecc 472	66.21	104.35
Ecc 572	61.46	109.92
Ecc 672	69.92	105.98

## REFERENCES

- Allen D. Eccentric muscle damage: mechanisms of early reduction in force. *Acta Physiol Scand* 2001;171:311-319.
- Arnold L, Henry A, Poron F, Baba-Amer Y, van Rooijen N, Plonquet A, Gherardi R, Chazaud B. Inflammatory monocytes recruited after skeletal muscle injury switch into anti inflammatory macrophages to support myogenesis. *J Exp Med*. 2007 May 14;204(5):1057–1069.
- Barton E, Morris L, Musaro a, Rosenthal N, Sweeney L. Muscle-specific expression of insulin-like growth factor I counters muscle decline in *mdx* mice. *J Cell Bio*. 2002 Apr 1;157(1):137-147.
- Barton-Davis E, Shoturma D, Sweeney H. Contribution of satellite cells to IGF-1 induced hypertrophy of skeletal muscle. *Acta Physiol Scand*. 1999 Oct 5;167:301-305.
- Beaton LJ, Tarnopolsky MA, and Phillips SM. Contraction-induced muscle damage in humans following calcium channel blocker administration. *J Physiol*. 2002 544:849-859.
- Bensaid W, Triffitt J, Blanchat C, Oudina K, Sedel L, Petite H. A biodegradable fibrin scaffold for mesenchymal stem cell transplantation. *Biomaterials*. 2003 24:2497-2502.
- Brickson S, Ji LL, Schell K, Olabisi R, St Pierre Schneider B, Best TM. M1/70 attenuates blood-borne neutrophil oxidants, activation, and myofiber damage following stretch injury. *J Appl Physiol*. 2003 Sep;95(3):969-76.
- Brooks S, Faulkner J. Contraction induce injury: recovery of skeletal muscles in young and old mice. *Am J Physiol* 1990 Mar;258(3 Pt 1):C436-42.
- Coolican S, Samuel D, Ewton D, McWade F, Florini J. The mitogenic and myogenic actions of insulin-like growth factors utilize distinct signaling pathways. *J Bio Chem*. 1997 Mar 7;272(10):6653-6662.
- Drinnan C, Zhang G, Alexander M, Pulido A, Suggs L. Multipmodal release of transforming growth factor- $\beta$ 1 and the BB isoform of platelet derived growth factor from PEGylated fibrin gels. *J Cont Release*. 2010 Apr 8;147:180-186.
- Eng C, Smallwood L, Rainiero M, Lahey M, Ward S, Leiber R. Scaling of muscle architecture and fiber types. *J Exp Bio* 2008;211:2336-2345.
- Faulkner J, Jones D, Round J. Injury of skeletal muscles of mice by forced lengthening during contractions. *Quart J Exp Physiol*. 1989;74:661-670.
- Fridén J, Lieber R. Eccentric exercise-induced injuries to contractile and cytoskeletal muscle fibre components. *Acta Physiol Scand*. 2001 Mar 17;1(3):321-6.

- Gonen-Wadmany M, Goldshmid R, Seliktar D. Biological and mechanical implications of PEGylating proteins into hydrogel biomaterials. *Biomaterials*. 2010 Jun 12;32:6025-6033.
- Hammers D, Merritt E, Matheny W, Adamo M, Walters T, Estep J, et al. " Functional deficits and insulin-like growth factor-I gene expression following tourniquet-induced injury of skeletal muscle in young and old rats. *J Appl Physiol*. 2008;105:1274-81.
- Hammers D, Sarathy A, Pham C, Drinnan C, Farrar R, Suggs L. Controlled release of IGF-1 from a biodegradable matrix improves functional recovery of skeletal muscle from ischemia/reperfusion. *Biotechnol Bioeng*. 2011 Nov 17. (*In press*)
- Hill M, Goldspink G. Expression and splicing of the insulin-like growth factor gene in rodent muscle is associated with muscle satellite (stem) cell activation following local tissue damage. *J Physiol*. 2003 Apr 11;549:409-418.
- Joya J, Kee A, Nair-Shalliker V, Ghoddusi M, Nguyen M, Luther P, Hardeman E. Muscle weakness in a mouse model of nemaline myopathy can be reversed with exercise and reveals a novel myofiber mechanism. *Hum Mol Gen*. 2004;13(21):2633-2645.
- Judge R, Dodd S. Oxidative damage to skeletal muscle following an acute bout of contractile claudication. *Atherosclerosis* 2003 Dec;171(2):219-224.
- Kandalla P, Goldspink G, Butler-Browne G, Mouly V. Mechano Growth Factor E peptide (MGF-E), derived from an isoform of IGF-1, activates human muscle progenitor cells and induces an increase in their fusion potential at different ages. *Mech Age Dev*. 2011 Feb 25;132:154-162.
- Kooijman R, Coppens A, Hooghe-Peters E. IGF-1 inhibits spontaneous apoptosis in human granulocytes. *Endocrinol* 2002 Apr;143(4):1206-1212.
- Liu H, Collins S, Suggs L. Three-dimensional culture for expansion and differentiation of mouse embryonic stem cells. *Biomaterials*. 2006;27:6004-6014.
- Masuro A, Giacinti C, Borsellino G, Dobrowolny G, Pelosi L, Cairns L, Ottolenghi S, Cossu G, Bernardi G, Battistini L, Molinaro M, Rosenthal N. Stem cell-mediated muscle regeneration is enhanced by ocal isoform oninsulin-like growth factor 1. *PNAS* 2004 Feb 3;101(5):1206-1210.
- Merritt E, Cannon M, Hammers D, Le L, Gokhale R, Sarathy A, Song TJ, Tierney M, Suggs L, Walters T, Farrar R. Repair of traumatic skeletal muscle injury with bone-marrow-derived mesenchymal stem cells seeded on extracellular matrix. *Tissue Eng Part A*. 2010 Sep;16(9):2871-81.
- Mourkioti F, Rosenthal N. IGF-1, inflammation and stem cells: interactions during muscle regeneration. *TRENDS Immuno*. 2005 Aug 15;26(10):535-542.

- Mosesson M. Fibrinogen and fibrin structure and functions. *J of Thromb Haemos*. 2005; 3(8):1894-1904.
- Pelosi L, Giancinti C, Nardis C, Borsellino G, Rizzuto E, Nicoletti C, Wannenes F, Battistini L, Rosenthal N, Molinaro M, Musaro A. Local expression of IGF-1 accelerates muscle regeneration by rapidly modulating inflammatory cytokines and chemokines. *J FASEB*. 2007;21:1393-1402.
- Pizza F, Peterson J, Baas J, Koh T. Neutrophils contribute to muscle injury and impair its resolution after lengthening contractions in mice. *J Physiol*. 2005 Feb 1;562(3):899-913.
- Sacks R and Roy R. Architecture of the hindlimb muscle of cats: functional significance. *J Morphol* 1982 Aug;173(2):185-195.
- Shapira-Schweitzer K, Seliktar D. Matrix stiffness affects spontaneous contraction of cardiomyocytes cultured within a PEGylated fibrinogen biomaterial. *Acta Biomater*. 2007;3:33-41.
- Talbot J, Morgan D. Quantitative analysis of sarcomere non-uniformities in active muscle following a stretch. *J Muscle Res Cell Motil*. 1996 Apr 17;2:261-268.
- Toumi H, Fguyer S, Best TM. The role of neutrophils in injury and repair following muscle stretch. *J Anat*. 2006 Apr;208(4):459-70.
- Warren G, Ingalls C, Lowe D, Armstrong R. Excitation-contraction uncoupling: major role in contraction-induced muscle injury. *Exerc Sport Sci Rev*. 2001 Apr 29;2:82-7.
- Wozniak A, Kong J, Bock E, Pilipowicz O, Anderson J. Signaling satellite-cell activation in skeletal muscle: markers, models, stretch, and potential alternate pathways. *Muscle Nerve*. 2005 Mar 31;3:283-300.
- Zhang B, Yeung S, Allen D, Qin L, Yeung E. Role of the calcium-calpain pathway in cytoskeletal damage after eccentric contractions. *J Appl Physiol*. 2008 Jul;105(1):352-7.
- Zhang G, Xiaohong W, Wang Z, Zhang J, Suggs L. A PEGylated fibrin patch for mesenchymal stem cell delivery. *Tissue Eng* 2006;12(1):9-19.
- Zhang G, Hu Q, Braunlin E, Suggs L, Zhang J. Enhancing efficacy of stem cell transplantation to the heart with a PEGylated fibrin biomatrix. *Tissue Eng Part A* 2008;14(6):1025-1036.



## **VITA**

Jessica Caitlin Treff was born on November 17, 1986 to parents, Ron and Jennifer Treff, in San Antonio, Tx. She was raised in Garland, Tx which afforded her the opportunity to attend North Garland High School and focus on human sciences. She graduated in May of 2005, and in the following August, enrolled at Hardin-Simmons University in Abilene, Tx. She majored in biology and received her Bachelor's of Science in May 2009. She attended The University of Texas-Austin in pursuit of a Master's of Science. Her thesis work was performed in the Muscle Physiology and Plasticity Lab in the department of Exercise Physiology. She received her Master's degree in December 2011.

Permanent address: 305 Thistle Dr.

Garland, Tx. 75043

This thesis was typed by Jessica Treff.